

# Oxygen distribution in AlN and Si<sub>3</sub>N<sub>4</sub> powders as revealed by chemical and spectroscopy techniques

J. Bermudo<sup>a</sup>, M.I. Osendi<sup>a,\*</sup>, J.L.G. Fierro<sup>b</sup>

<sup>a</sup>*Instituto de Cerámica y Vidrio, CSIC, Crta. Antigua Valencia Km- 24.3, Arganda del Rey, 28500, Madrid, Spain*

<sup>b</sup>*Instituto de Petroleoquímica y Catálisis, CSIC, Universidad Autónoma, Cantoblanco, Madrid, Spain*

Received 1 February 1999; received in revised form 2 February 1999; accepted 7 April 1999

## Abstract

The oxygen content and the surface composition of pure AlN and Si<sub>3</sub>N<sub>4</sub> powders, synthesized by SHS reactions and commercial routes, have been studied using X-ray photoelectron spectroscopy (XPS) and hot gas extraction techniques. Surface stoichiometry is identified and discussed for each powder. The AlN and Si<sub>3</sub>N<sub>4</sub> powders synthesized by SHS technology were subjected to a sputtering process with rare gas bombardment (Ar<sup>+</sup>) in order to progressively remove the uppermost layers. A gradient in the oxygen distribution between the particle surface and the interior was measured. Differences in the oxygen distribution for the AlN and Si<sub>3</sub>N<sub>4</sub> powders depending on the route of synthesis have been observed. © 2000 Elsevier Science Ltd and Techna S.r.l. All rights reserved.

**Keywords:** Oxygen distribution; AlN and Si<sub>3</sub>N<sub>4</sub> powders; Chemical and spectroscopic techniques

## 1. Introduction

The AlN and the Si<sub>3</sub>N<sub>4</sub> materials are currently used in a number of industrial and technological applications. These materials are competitive candidates to substitute the more traditional materials due to their intrinsic properties: the good mechanical performance in the case of Si<sub>3</sub>N<sub>4</sub>, and high thermal conductivity for the AlN materials.

Specifically, aluminum nitride (AlN) is a very attractive substrate for applications in electronic packaging due to its high thermal conductivity (320 W/mK), close to thermal conductivity of metals [1,2], high electrical resistivity (10<sup>11</sup>–10<sup>14</sup> Ω cm) and a thermal expansion coefficient (4.3–4.5×10<sup>-6</sup>/°C) matched to that of semiconductor silicon. The existence of bulk oxygen within the AlN grains influences its thermal conductivity [3], and furthermore the stoichiometry of the oxygen compounds on the powder surface will affect the bonding between the AlN used as substrate and the metal traditionally used in the fabrication of electronic devices [4].

On the other hand, silicon nitride (Si<sub>3</sub>N<sub>4</sub>) due to the strength of its highly covalent bond has an excellent set of intrinsic properties such as: mechanical strength at room and high temperatures [5,6], high toughness [7] and low coefficient of thermal expansion. These properties and its low density encourages the use of Si<sub>3</sub>N<sub>4</sub> materials in areas where the metals have been used largely [8], since the performance of metal components is highly limited by the temperature of work. Generally, an important amount (≈10% by weight) of additives, usually oxides, are required to promote sintering in silicon nitride [9]. In fact, the brilliant properties associated to the Si<sub>3</sub>N<sub>4</sub> materials are conditioned by the composition of the secondary phase and the final microstructure. The composition of this secondary phase will depend on the presence of oxygen on the surface of the powders as well as the amount and type of additives used for sintering [10]. Some studies have pointed out the relationship between the oxygen content in the Si<sub>3</sub>N<sub>4</sub> powders and the strength of the final material [11].

In spite of the better properties associated with the use of AlN and Si<sub>3</sub>N<sub>4</sub> materials, some problems have to be overcome before massive use in industrial applications. One of the main problems to implement the use of both materials is the high production cost associated to

\* Corresponding author. Tel.: +349-91-871-1800, fax: +349-91-870-0550.

E-mail address: miosendi@icv.csic.es (M.I. Osendi).

the use of  $\text{Si}_3\text{N}_4$  and  $\text{AlN}$  components compared to the cost of metals and the alumina substrates, respectively. Self-propagating high-temperature synthesis (SHS) uses the energy obtained from high exothermic reactions, and therefore reduces costs in the synthesis of  $\text{AlN}$  and  $\text{Si}_3\text{N}_4$  powders [12,13]. Nevertheless, validation of the SHS technology as a competitive route will depend not only on the economic results but also on the physical and chemical properties of the products obtained using this route.

In the present research, powders of  $\text{AlN}$  and  $\text{Si}_3\text{N}_4$  synthesized by SHS reactions have been compared to commercially available powders, in order to elucidate possible differences in the surface chemistry depending on the route of synthesis. Accordingly X-ray photoelectron spectroscopy (XPS) was selected as the most adequate technique to analyze these differences.

## 2. Experimental

The powders employed have been obtained from different sources. The reference powders were:  $\text{AlN}$  (grade B), and  $\text{Si}_3\text{N}_4$  (LC 12-SX), both of Hermann C. Starck (Germany). The powders synthesized by the SHS technology have been developed by SHS-España, and will be labeled as  $\text{AlN-SHS}$  and  $\text{Si}_3\text{N}_4\text{-SHS}$ . As reported in a previous work [14], metallic contaminants were less than 0.1 wt% in all the powders except the  $\text{Si}_3\text{N}_4\text{-SHS}$  which showed a relatively high level of Fe (0.1 wt%).

Measurements of the total oxygen content were done using a commercial hot gas extraction equipment (Leco, EF-400). The specific surface area of the powders was measured at the liquid nitrogen temperature, using the BET method (Monosorb MS-13) and the particle size distribution was determined by laser scattering using a particle size analyzer (Coulter LS 130). Metal impurities in each powder were determined by inductively coupled plasma spectrometry (Jobin Ivon 38 P).

The amount of surface oxygen in the powders was measured by X-ray photoelectron spectroscopy (XPS). Spectra were acquired with a ESCALAB 200 R electron spectrometer provided with a hemispherical electron analyzer and a  $\text{Al } K_\alpha$  ( $h\nu = 1486.6$  eV) X-ray exciting source working at 120 W.  $\text{C}_{1\text{S}}$ ,  $\text{O}_{1\text{S}}$ ,  $\text{N}_{1\text{S}}$  and  $\text{Al}_{2\text{p}}$  or  $\text{Si}_{2\text{p}}$  peaks were recorded for each sample. The pass energy was fixed at 10 eV, which enables good resolution at reasonable acquisition times. Each spectral region was signal-averaged for 50–100 scans, depending on the intensity of the signal, in order to obtain good signal to noise ratios. Atomic ratios were computed from the intensity ratios and published atomic sensitivity factors. The intensity of the peaks was calculated by integration of peak areas after subtraction of an S-shaped background and fitting the experimental curve to a sum of Gaussian and Lorentzian curves of a G/L proportion

15–35%. The binding energies (BE) were calculated relative to  $\text{C}_{1\text{S}}$  peaks at 284.9 eV.

In addition, the powders synthesized by SHS were subjected to a sputtering process under  $\text{Ar}^+$  (3 keV) bombardment for 10 min, in order to remove the first atomic layers. Then XPS was performed again after these times, in order to quantify the normalized oxygen content and the atomic ratios ( $\text{O}/\text{Al}$ ,  $\text{O}/\text{Si}$ ) in the inner parts of the grains. These conditions allowed the removal of 8–10 Å per min on the surface of the powders [16].

## 3. Results and discussion

### 3.1. $\text{AlN}$ powders

The characteristic metal impurities, average particle size, specific surface area and oxygen content of the synthesized SHS powders ( $\text{Si}_3\text{N}_4$ ,  $\text{AlN}$ ), and the reference commercial powders are detailed in Table 1.

The commercial powders have larger oxygen content, showing at the same time lower grain size and higher specific surface area than the respective SHS powders. As oxygen impurities come mainly from oxidation of the particles in contact with the atmosphere, they have to be related to the specific surface area of the powders.

Binding energies (BE) calculated for the  $\text{O}_{1\text{S}}$ ,  $\text{Al}_{2\text{p}}$  and  $\text{N}_{1\text{S}}$  core levels in the two  $\text{AlN}$  powders are shown in Table 2. The BE and the atomic rates on the surface were calculated by deconvolution of the spectral peaks for each orbital [16,17] as represented in Fig. 1. The corresponding stoichiometry, also indicated in the table, was determined according to the tabulated values for the atomic sensitivity factors of the orbitals  $\text{O}_{1\text{S}}$ ,  $\text{Al}_{2\text{p}}$  and  $\text{N}_{1\text{S}}$  [17].

Observation of one or two  $\text{O}_{1\text{S}}$  components in the XP spectra is conclusive of the presence of oxidic species. It should be noticed that binding energies associated to the  $\text{Al}_{2\text{p}}$  and  $\text{O}_{1\text{S}}$  orbitals increase when the number of oxygen atoms in the surrounding aluminum atoms increases. This situation can be explained by the decrease in the electronic density around the aluminum

Table 1

Physical and chemical characteristics: metal contaminants, total oxygen content, grain size ( $d_{50}$ ) and  $S_{\text{BET}}$  ( $\text{m}^2/\text{g}$ )

	O (wt%)	C (wt%)	Metals (%)	$d_{50}$ ( $\mu\text{m}$ )	$S_{\text{BET}}$ ( $\text{m}^2/\text{g}$ )
$\text{AlN}$ grade B <sup>a</sup>	1.7	0.06	< 0.1	0.5	3.6
$\text{AlN-SHS}$ <sup>b</sup>	0.9	0.2	< 0.1	16	0.7
$\text{Si}_3\text{N}_4$ HC-L12 <sup>a</sup>	2.0	0.1	< 0.1	0.7	21
$\text{Si}_3\text{N}_4\text{-SHS}$ <sup>b</sup>	1.2	0.1	< 0.2	10	3.5

<sup>a</sup> Starck.

<sup>b</sup> SHS-España.

Table 2

BE for the orbitals ( $O_{1s}$ ,  $Al_{2p}$ ,  $N_{1s}$ ) and chemical species on the surfaces of the AlN powders

	BE $O_{1s}$ (eV)	Species	BE $Al_{2p}$ (eV)	Species	BE $N_{1s}$ (eV)	Species
AlN (grade B)	530.9 (73%)	$AlO_xN_y$	73.8 (58%)	AlN	397.3 (91%)	AlN
	532.2 (27%)	$Al_2O_3$	74.6 (42%)	$AlO_xN_y$ , $Al_2O_3$	398.3 (9%)	AlON
AlN-SHS	531.8	$Al_2O_3$	73.6 (75%)	AlN	396.7	AlN
			74.6 (25%)	$Al_2O_3$		

atom, due to the higher electronegativity of the oxygen atoms. This enhances electrostatic interactions between the aluminum nuclei and the electrons [22], which produces the higher BE detected in the  $O_{1s}$  and  $Al_{2p}$  orbitals.

Table 2 shows that for AlN-SHS the BE of the  $Al_{2p}$  orbital has two values: 73.6 and 74.6 eV, respectively associated to two compounds: 75% of the atoms as AlN and 25% of the atoms as  $Al_2O_3$ . In the commercial AlN, the  $Al_{2p}$  orbital also shows two components: 73.8 eV, 74.6 eV, whose corresponding proportion are 58% of the Al atoms as AlN and the remaining 42% forming oxidic components. By combining the BE values of both  $O_{1s}$  and  $Al_{2p}$  core-levels it is evident that  $AlO_xN_{1-x}$  and

$Al_2O_3$  species, with the former dominant, are present on the surface of this powder.

The existence of different surface stoichiometries in the aluminum nitrides studied seems to depend on the route of synthesis. As above stated, the peak areas from the spectra lines associated to each orbital can be used to obtain quantitative data. Accordingly in Table 3 the O/Al and N/Al atomic ratios are summarized. These results reveal a higher oxygen concentration, and lower N, in the surface of AlN-SHS powder than in the commercial one. But according to the results of Table 1, the total oxygen content is higher in the commercial AlN (1.7 wt%) than in the SHS (0.9 wt%); hence commercial powder must have a higher amount of oxygen in the subsurface. It should be recalled that to get high conductivity AlN materials the oxygen level inside the grains must be kept at a minimum [18,19].

### 3.2. $Si_3N_4$ powders

The binding energies of core-levels of both silicon nitride powders are summarized in Table 4. Deconvolution of respective spectral peaks is shown in Fig. 2. The BE of the orbital  $O_{1s}$  in the commercial  $Si_3N_4$  has a value of 532.4 eV and considering the tabulated BE [15] the specie associated to this energy is  $SiO_xN_x$ . For the  $Si_3N_4$ -SHS, the BE in orbital  $O_{1s}$  is 532.7 eV and the associated [15] specie is  $SiO_2$ . In this powder the increase in the BE with a higher number of oxygen atoms is also observed. The analysis of the BE associated to the orbital  $Si_{2p}$  (Table 4) identified oxidic components for both powders, associated to  $SiO_2$  and  $SiO_xN_x$  species; in agreement with the components identified from the analysis of the BE in the  $O_{1s}$  orbital (Table 4). Similarly, the BE obtained from the orbital  $N_{1s}$  in both powders allows also identification of  $Si_3N_4$  and  $SiO_xN_x$  species, in agreement with the data

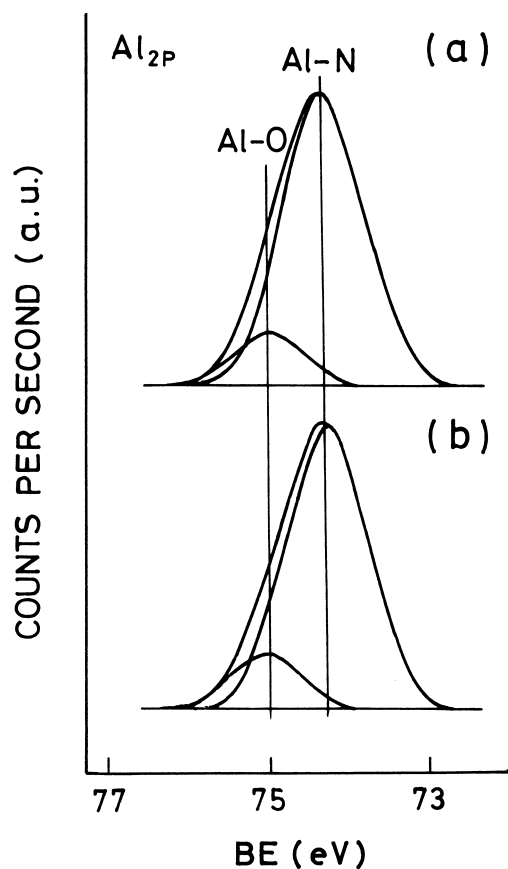


Fig. 1.  $Al_{2p}$  core level spectra of the aluminum nitride powders: (a) commercial and (b) SHS.

Table 3

O/Al and N/Al atomic ratios in the AlN

	(O/Al)	N/Al
AlN (grade B)	0.36	0.94
AlN-SHS	1.81	0.33

Table 4

BE for the orbitals ( $O_{1s}$ ,  $Si_{2p}$ ,  $N_{1s}$ ), percentage and species on the surfaces of the  $Si_3N_4$  powders studied

	$O_{1s}$ (eV)	Species	$Si_{2p}$ (eV)	Species	$N_{1s}$ (eV)	Species
$Si_3N_4$ (LC-12)	532.4	$SiO_xN_y$	101.6 (72%)	$Si_3N_4$ $SiO_xN_y$	397.6 (80%)	$Si_3N_4$ $SiO_xN_y$
			102.6 (28%)		398.6 (20%)	
$Si_3N_4$ -SHS	532.7	$SiO_2$	101.5 (76%)	$Si_3N_4$	397.4	$Si_3N_4$
			103.1 (24%)	$SiO_2$		

obtained from the previous analysis of the BE of the  $O_{1s}$  and  $Si_{2p}$  orbitals.

The O/Si and N/Si atomic ratios calculated from the deconvolution of the spectral peaks are reflected in Table 5. A higher oxygen content on the surface of the  $Si_3N_4$ -SHS powders than in the commercial ones is observed, as occurred with both AlN powders. Hence, the total oxygen content (Table 1) for the commercial  $Si_3N_4$  (1.7 wt%) was higher and conversely the surface oxygen seems lower (Table 5), it can be inferred that oxygen content inside the particles should be higher in this powder than in the SHS powders. Besides, this higher oxygen concentration on the surface can act as a barrier, to avoid further penetration towards the inside of the particle.

### 3.3. Oxygen distribution

The previous results show that in AlN and  $Si_3N_4$  synthesized by the SHS method oxygen concentrates predominantly on the surface of the powders. To investigate the alteration of this concentration towards the interior of the particles, XPS have been analyzed after sequential removal of the uppermost surface layers by  $Ar^+$  bombardment. The atomic ratios after 5 and 10 min sputtering on the AlN-SHS are listed in Table 6, and the results obtained after the same process performed on the  $Si_3N_4$ -SHS are listed in Table 7.

The results of Table 6 show a fast decrease in the amount of oxygen present at the outer surface layers.

Table 5

O/Si and N/Si atomic ratios in the  $Si_3N_4$  powders

	(O/Si)	N/Si
$Si_3N_4$ (LC-12)	0.28	1.35
$Si_3N_4$ -SHS	0.69	1.05

Table 6

Atomic ratio (O/Al) on the surface and after 5 and 10 min sputtering in the AlN SHS

	O/Al
AlN-SHS (surface)	1.81
AlN-SHS (4–5 nm deep)	0.52
AlN-SHS (8–9 nm deep)	0.04

The (O/Al) atomic ratio changes from 1.81 to 0.04 between the surface and the lowest layer analyzed. The (O/Al = 1.81) atomic ratio determined on the surface is between that of  $Al_2O_3$  (O/Al = 1.5) and  $AlOOH$  (O/Al = 2). The measured binding energies for the  $Al_{2p}$  and  $O_{1s}$  orbitals (Table 2) are very close to the BE of these compounds; therefore, the oxidic components covering the surface of the powders will be a mixture of  $Al_2O_3$  +  $AlOOH$ , in agreement with the description of Ponthieu et al. [21]. The results obtained on the AlN-SHS powders suggest that oxygen concentrates on the surface of the aluminum nitride powder, according with the results of Müller et al. [20,21]. Nevertheless, these authors observed that oxygen concentrated in a surface layer of 2 nm thickness, while in the AlN-SHS powders investigated this layer had 8–10 nm of thickness. The results for the  $Si_3N_4$ -SHS (Table 7) show the same behavior detected for the AlN-SHS (Table 6). The O/Si atomic ratio decreases from a value of 0.69 to 0.04 between the surface and the interior of the  $Si_3N_4$  particles. The higher amount of oxygen in the silicon nitride powders is located in a surface layer of  $\approx 8$  nm thickness. This result disagrees with several results published in the literature. The thickness obtained by Okada et al. [22] for the oxidized layer was between 0.4 and 1 nm, while Peuckert [23] considered a minimum oxygen content located on the surface of the silicon nitride grains, and a thickness for the external oxidized layer of  $\approx 2$  nm. Raider et al. [24] deduced an external layer 3–5 nm thick where the oxygen was located. The results obtained in the present work indicate most of the oxygen atoms concentrate on the surface of the silicon nitride particles, over a layer 8–10 nm thick. One possible reason for the dispersion in the values for the external oxidized layer could be its dependence on the route of synthesis and on their surface area. Aluminum nitride powders obtained by SHS showed a notably higher oxidation degree on

Table 7

Atomic ratio (O/Si) on the surface and after 5 and 10 min sputtering in the  $Si_3N_4$  SHS

	O/Si
$Si_3N_4$ -SHS (surface)	0.69
$Si_3N_4$ -SHS (4–5 nm deep)	0.46
$Si_3N_4$ -SHS (8–9 nm deep)	0.04

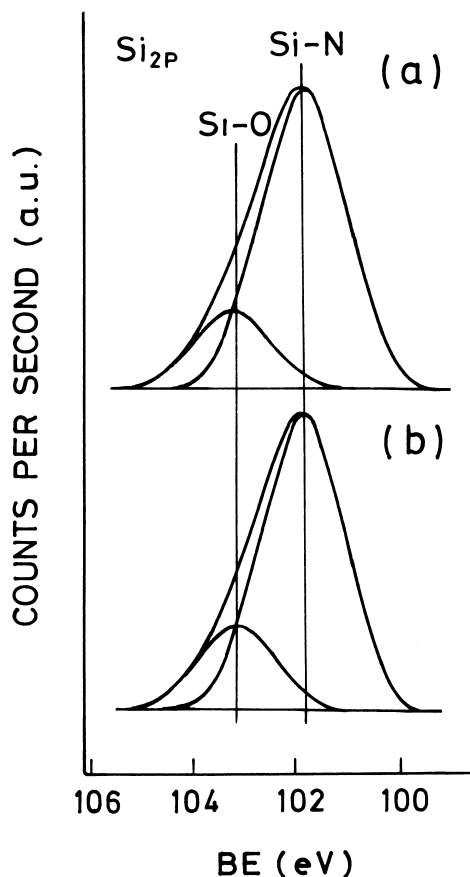


Fig. 2.  $\text{Si}_{2p}$  core level spectra of silicon nitride powders: (a) commercial and (b) SHS.

the surface when compared to the  $\text{Si}_3\text{N}_4$ -SHS powders, though the last had a higher specific surface area. The important data supply by the sputtering process carried out is the possibility to measure the real oxygen content beneath the surface, detecting the decrease in oxygen amount for a controlled depth inside the particles.

#### 4. Conclusions

The oxygen content and distribution have been studied beneath the surface in the aluminum nitride and silicon nitride powders obtained by SHS routes. The powders synthesized by SHS reactions presented a higher oxygen concentration on the surface than the commercial powders used as reference. The oxidized zone was confined in a surface layer of 8–10 nm thickness. This highly oxidized surface seems to act as passivating surface, avoiding further oxidation of the particle interior. Oxygen enrichment on the surface of the powders was always higher in the AlN powders than in the  $\text{Si}_3\text{N}_4$  powders for both SHS and commercial products.

#### Acknowledgements

This work has been financially supported by the Project Prometheus (Spain) and by the CICYT (Spain), reference MAT97-708.

#### References

- [1] D. Suryanarayana, Thermally conductive ceramics in electronic packaging, *J. Electron. Packag.* 111 (1989) 192.
- [2] M.P. Borom, G.A. Slack, J.W. Szymaszek, Thermal conductivity of commercial AlN, *Ceram. Bull.* 51 (11) (1972) 852.
- [3] A.V. Virkar, T.B. Jackson, R.A. Cutler, Thermodynamic and kinetics effects of oxygen removal on the thermal conductivity of AlN, *J. Am. Ceram. Soc.* 72 (11) (1989) 2031–2042.
- [4] P. Kluge-Weiss, J. Gobrecht, Directly bonded copper metallization of AlN substrates for powder hybrids, *Mater. Res. Soc. Symp. Proc.* 40 (1985) 399.
- [5] H. Takahashi, N. Shinohara, K. Uematsu, T. Junichiro, Influence of granule character on the mechanical properties of sintered silicon nitride, *J. Am. Ceram. Soc.* 79 (4) (1996) 843–848.
- [6] A.E. Pasto, S. Nathansohn S., Development of improved processing methods for silicon nitride ceramics, ASME Paper 91-GT-316, presented at the international Gas Turbine and Aero-engine Congress and Exposition, Orlando, FL, 3–6 June 1991.
- [7] S.R. Choi, J.A. Salem, Crack-growth resistance of in situ-toughened silicon nitride, *J. Am. Ceram. Soc.* 77 (4) (1994) 1042–1046.
- [8] L.Y. Russell, Know Oh-Hun, Silicon nitride for heat engine and bearing components, in: I. Birkby (Ed.), *Ceramic Technology International*. Sterling Publications Ltd, UK, 1996, pp. 21–24.
- [9] Y.G. Gogotsi, G. Grathwohl, Stress enhanced oxidation of silicon nitride ceramics, *J. Am. Ceram. Soc.* 76 (12) (1993) 3093–3104.
- [10] M.J. Hoffmann, High-temperature properties of  $\text{Si}_3\text{N}_4$  ceramics, *MRS Bulletin*, February 1995.
- [11] S. Nathanson, A.E. Pasto, W.J. Rourke, Effect of powder surface modifications on the properties of silicon nitride ceramics, *J. Am. Ceram. Soc.* 76 (9) (1993) 2273–2284.
- [12] K.A. Golubjatnikov, G.C. Stangle, R.M. Spriggs, The economics of advanced self-propagating high-temperature synthesis materials Fabrication, *Am. Ceram. Soc. Bull.* 72 (12) (December 1993).
- [13] A.G. Merzhanov, History and recent developments in SHS: review paper, *Ceram. Int.* 21 (1995) 371–379.
- [14] J. Bermudo, M.I. Osendi, Study of AlN and  $\text{Si}_3\text{N}_4$  powders synthesized by SHS reactions, *Ceram. Int.* 25 (7) (1999) 607–612.
- [15] G.E. Muilenberg, Handbook of X-ray photoelectron spectroscopy, Perkin Elmer, Physical Electronics Division, Eden Prairie, MA, 1979.
- [16] J. Bermudo, Estudio de materiales de nitrato de silicio y nitrato de aluminio procesados mediante polvos obtenidos por reacciones de autocombustion, Universidad de Alcalá de Henares, Madrid, Spain, 1996.
- [17] D.P. Woodruff, T.A. Delchar, Modern techniques of surface science, Cambridge University Press 1986.
- [18] K. Ishizaki, K. Watari, T. Fujikawa, Thermal conduction mechanism of aluminum nitride ceramics, *J. Mater. Sci.* 27 (1992) 2627–2630.
- [19] K. Watari, M. Kawamoto, K. Ishizaki, Sintering chemical reactions to increase thermal conductivity of aluminum nitride, *J. Mater. Sci.* 26 (1991) 4727–4732.
- [20] A. Thomas, G. Müller, Determination of the oxygen dissolved in the AlN lattice by hot gas extraction from AlN ceramics, *J. Eur. Ceram. Soc.* 8 (1991) 11–19.
- [21] E. Ponthieu, P. Grange, B. Delmon, L.L. Lonnoy, R. Bechara, J. Grimblot, Proposal of a composition model for a commercial AlN Powders, *J. Eur. Ceram. Soc.* 8 (1991) 233–241.

- [22] K. Okada, K. Fukuyama, Y. Kameshima, Characterization of surface-oxidized phase in silicon nitride and silicon oxinitride powders by X-ray photoelectron spectroscopy, *J. Am. Ceram. Soc.* 78 (8) (1995) 2021–2026.
- [23] M. Peuckert, P. Greil, Oxygen distribution in silicon nitride powders, *J. Mater. Sci.* 22 (1987) 3717–3720.
- [24] I. Raider, J.A. Flitsch, W.A. Aboaf Piskin, Surface oxidation of silicon nitride films, *J. Electrochem. Soc.* 123 (4) (1976) 560–565.